Charging and Mobilization of Dust Particles on a Surface in Plasma

José H. Pagán Muñoz,[1,2,*] Xu Wang,[1,2] Mihály Horányi,[1,2] Vladimir Kvon,[3] Luuk Heijmans,[3] Manis Chaudhuri,[3] Mark van de Kerkhof,[3] Andrei M. Yakunin,[3] Pavel Krainov,[4] and Dmitry Astakhov[4]

[1]*NASA SSERVI's Institute for Modeling Plasma, Atmospheres and Cosmic Dust (IMPACT), University of Colorado, Boulder, Colorado 80303, USA*

[2]*Laboratory for Atmospheric and Space Physics (LASP), University of Colorado, Boulder, Colorado 80303, USA*

[3]*ASML, Eindhoven, The Netherlands*

[4]*ISTEQ B.V., High Tech Campus 9, 5656 AE Eindhoven, The Netherlands*

(Received 10 April 2024; revised 6 June 2024; accepted 8 August 2024; published 11 September 2024)

We present first experimental results showing that single dust particles on a dielectric surface are mobilized and lofted due to exposure to an electron beam or ultraviolet radiation. It is shown that secondary electrons and/or photoelectrons emitted from a substrate surface are recollected on the surfaces within microcavities between a dust particle and the substrate surface, resulting in large negative charges and subsequently causing mobilization of the dust particle due to Coulomb repulsion. Dust mobility tested against the electron beam energy is shown to follow the secondary electron yield curve of the substrate surface in both the experimental and modeling results. The results verified the role of emitted electrons from the substrate surface in charging and mobilization of single dust particles.

DOI: 10.1103/PhysRevLett.133.115301

Charging of dust particles and their subsequent mobilization, lofting, and transport have been known to cause various issues in both terrestrial and extraterrestrial applications. In semiconductor manufacturing, dust particles fall on photomasks in lithography [1] or on wafers during plasma processing [2], causing defects and even failures in chip production. Flaky dust particles are recorded to transport in fusion reactors [3], causing contamination and even disruption of the reactors. Dust particles are identified to interact with high-energy proton or electron beams in particle accelerators, causing beam losses [4–6]. In space, electrostatic dust transport is a more than five-decade old problem related to observations of the lunar horizon glow [7,8], the dust ponds on asteroid 433 Eros [9,10], and the spokes in Saturn's rings [11,12]. Additionally, charged dust particles pose challenges to long-term human and robotic exploration on the surfaces of the Moon and asteroids [13]. To solve these issues, studying dust charging, mobilization, and lofting has attracted an increased interest over the past decades.

Previous charging theories are mainly based on macroscale plasma sheath theories. A simple shared charge model treats dust particles to be part of the substrate surface. The surface charge is determined by the sheath electric field, which is scaled by the Debye length [14]. However, the charge and subsequent electric force of dust particles is found to be too small to overcome the adhesive and/or gravitational force to lift the dust particles off the surface [15,16]. Because of the stochastic process of electrons and ions arriving at a surface at random time intervals, the charge accumulated on dust particles fluctuates over time. A charge fluctuation theory [15,17] shows that dust particles have increased possibility to be mobilized or even lofted when their charge fluctuates to the maximum magnitudes. However, these models are unable to explain experimental demonstrations of dust mobilization and lofting in the laboratory [16,18,19] and possible lofting indicated from the space observations [7–12]. Specifically, the charge predicted by these models is off by several orders of magnitude to explain possible dust lofting from the lunar surface [16].

A patched charge model (PCM) [16] has advanced the fundamental understanding of dust charging and lofting from a dusty surface, such as the regolith of the moon and asteroids. In contrast to previous macroscale models, the PCM describes a charging process within microcavities formed between dust particles. The size of the microcavities can be approximated to be the size of dust particles (on the order of nm to μm), much smaller than the Debye length for typical laboratory and space plasma conditions (on the order of mm to m) [16]. The PCM shows that secondary electrons and/or photoelectrons are emitted when an electron beam and/or ultraviolet (UV) light hits a dusty surface, and some of these emitted electrons are reabsorbed by the microcavities, depositing negative charges on the surfaces of the surrounding particles. Because of the small size of the microcavities, a small potential difference across the cavity creates a large electric field with substantial negative charges accumulated on the surrounding

*Contact author: Jose.Pagan@lasp.colorado.edu

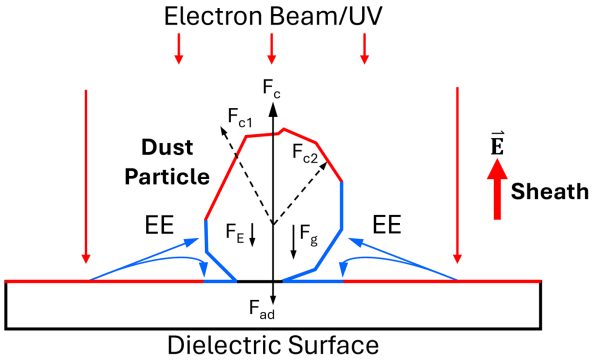

FIG. 1. Patched charge model for a single particle (PCM-SP) on the surface. A dielectric dust particle rests on a dielectric substrate surface. The red patches are charged by direct exposure to an electron beam or UV. Secondary electrons and/or photoelectrons are emitted from the substrate surface, and some of these emitted electrons (EE) are re-deposited on the blue patches within microcavities between the dust particle and substrate surface, resulting in enhanced negative charges. Forces exerted on the dust particle include F_c: the Coulomb repulsive force, F_{ad}: the adhesive force, F_g: the gravitational force, and F_E: the sheath electric field force. F_c is the vector sum of F_{c1} and F_{c2}.

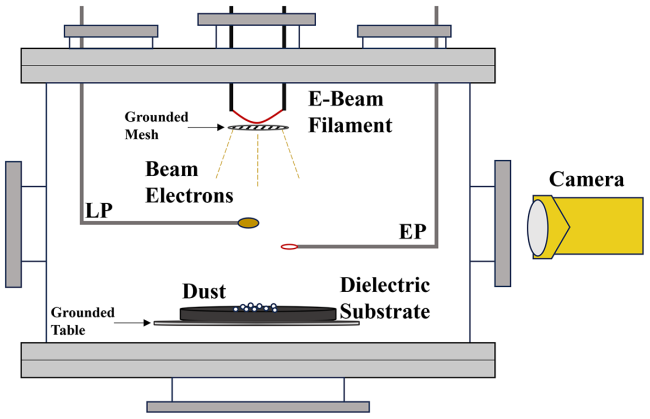

FIG. 2. Schematic of the experimental setup. Dust particles are exposed to an electron beam generated from a hot filament at the top of the chamber or a UV source (not shown). Dust mobilization is recorded using a video camera. A Langmuir probe (LP) and an emissive probe (EP) are used to characterize the plasma and the substrate surface potential.

particles according to Gauss's law. Subsequently, the strong Coulomb repulsion between these negatively charged particles causes them to be lofted or mobilized. The PCM is validated by a series of follow-up laboratory experiments [16,20–23].

In addition to dusty surfaces that have multiple layers of dust on the surface, in many cases as described in the beginning of the paper, dust particles directly rest on a solid surface. Charging and mobilization of single dust particles on the surface remains poorly understood. Simulations [24] show that a dust particle resting on a flat surface can collect additional electrons on the side surface of the particle, resulting in enhanced charge. Recent simulations [1] show charge accumulation of secondary electrons within gaps between a spherical particle and the substrate surface, which may be sufficient to cause dust to be lofted. Based on previous studies [1,16], here we introduce a complete charge model extending the PCM for single particles (PCM-SP) and validate it with both experimental and modeling results that show mobilization and lofting of single dust particles on a dielectric surface due to exposure to an electron beam or UV radiation.

Figure 1 shows a single dust particle resting on a solid surface exposed to an electron beam or UV. Gaps between the curved surfaces of the particle and the flat substrate create microcavities. The red patches are directly exposed to the electron beam or UV, and their charge is determined by the sheath electric field formed above the surface. When the electron beam or UV hits the substrate surface, secondary electrons or photoelectrons are generated, and some of them are reabsorbed by the microcavities, depositing negative charges on the bottom surface areas (blue patches) of the dust particle, which are in the shadow of the beam or UV light. The resulting negative potential returns the secondary electrons or photoelectrons with lower energies, which are collected by the underneath substrate surface within the cavities, accumulating negative charges on them (blue patches) as well.

The electric field within the microcavities is large due to the small size of the microcavities (on the order of nm to μm), resulting in substantial negative charge deposition on the blue patch surface area. Subsequently, as shown in Fig. 1, the strong Coulomb repulsive forces (F_c) between the negatively charged blue patches on the dust particle and substrate surface overcome the total force of the adhesive force F_{ad}, the gravitational force F_g, and the sheath electric field force F_E, causing the particle to be mobilized or lofted.

To verify the PCM-SP charging model, experiments were carried out in a cylindrical vacuum chamber, 30 cm tall and 44 cm in diameter (Fig. 2). The chamber pressure was $\sim 10^{-6}$ torr. An electron beam source was at the top of the chamber. The beam was generated by thermionic electrons released from a hot filament and accelerated by the negative voltage on the filament with respect to a grounded mesh. The beam energy was varied between 30 and 500 eV. A UV lamp (172 nm wavelength and 7.2 eV photon energy) was used as an alternative charging source in the experiment.

Irregularly shaped SiO_2 dust particles were dispersed on a dielectric kapton film (25 μm thick). The kapton film was laid on a delrin plate which is 15 cm in diameter and 2.6 cm thick. The substrate was ~15 cm from the beam or UV source. Utilizing the empirical equation for the extrapolated range of the electron energy [25], we conclude that the electron beam in our experiment with the maximum penetration depth of 0.106 μm does not penetrate past

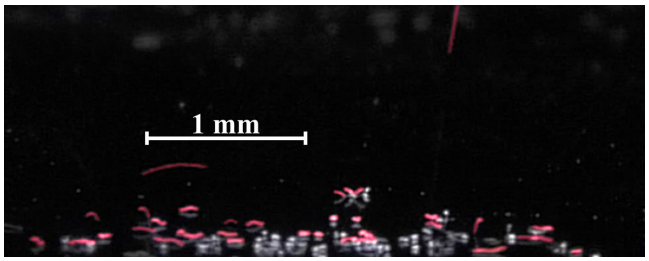

FIG. 3. Recorded still image showing hopping and lofting (red lines) of dust particles on the surface under an electron beam exposure.

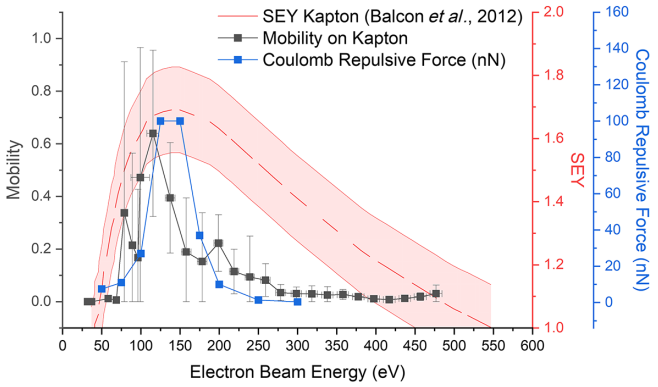

FIG. 4. Dust mobility (experimental) and the dust repulsive force (modeling) on the kapton surface as a function of the electron beam energy. An SEY curve for kapton [26] is overplotted. The dashed line shows the average SEY value with errors shown in the shaded area.

the 25 μm thick kapton film. The underneath delrin plate is thus not expected to affect the secondary electron emission from the kapton film. The dust particles had a size distribution of less than 45 μm in diameter (datasheet from MSE Supplies). Dust mobilization and lofting was recorded using a video camera at 60 frames/sec and 1920×1080 pixel resolution.

A double-sided Langmuir probe and an emissive probe were used to characterize the plasma conditions and electric potentials above the substrate surface. The Langmuir probe consisted of two 0.635 cm diameter planar probes facing back to back and electrically isolated from each other. The bottom probe, which does not see the electron beam, was used to characterize the thermal electrons in the middle of the chamber ~6 cm from the surface. At a height of ~0.5 cm, the top probe was used to measure the energy and current density of the electron beam reaching the surface to determine its effects on dust charging and mobility. The emissive probe was used to characterize the substrate surface potential.

The recorded videos confirm that individual dust particles mostly hop around on the surface and a few are lofted to higher heights above the surface under the electron beam exposure (Fig. 3). Some of the hops are too small to be differentiated from rolling or sliding on the surface. The exact physical processes that determine rolling or sliding vs hopping or lofting, as shown in Fig. 1, have yet to be investigated. A possible explanation is that the irregular shape of the jagged dust particles and the nonuniformity of the electron beam incident on the dust particles and the substrate surface result in uneven horizontal Coulomb repulsive forces, causing the particles to roll or slide on the surface. When the vertical repulsive force overcomes the downward pointing "negative" forces (i.e., $F_c > F_{ad} + F_g + F_E$ as shown in Fig. 1), the particles are lofted or hop.

Nevertheless, dust mobility was analyzed by pixel shifting between each successive frame. A high contrast between the dust and substrate is created, thus pixels with brightness above a designated threshold were considered dust particles. A pixel that changes in brightness between successive frames was counted as a single pixel shift. Mobility was determined by the sum of the pixel shifts divided by the total amount of the pixels counted as dust particles in the whole frame. Finally, the dataset of all data points in the experiment was normalized to its highest value to produce a mobility plot.

Dust mobility as a function of the beam energy is shown in Fig. 4, in which the modeling results of the repulsive force between a dust particle and the substrate surface for the same conditions as in the experiment are also shown and described in detail later. For each beam energy, three trials were performed, resulting in error bars shown in the figure. The beam energy reaching the surface was corrected using the difference between the beam energy at source and the substrate surface potential. The mobility of the particles starts when the beam energy becomes larger than ~70 eV, increases rapidly with the beam energy and hits the peak at ~125 eV, then decreases at a slower rate, and finally ceases when the beam energy is larger than ~320 eV.

Based on the PCM-SP, dust mobility is determined by Coulomb repulsion between negatively charged surfaces on a dust particle and the substrate due to reabsorption of secondary electrons within their microcavities. It is thus expected that dust mobility correlates with the secondary electron yield (SEY).

An SEY curve measured for a kapton film [26] is overplotted in Fig. 4, showing the SEY larger than 1 for the beam energy of 50–550 eV. Vertical potential profiles above the kapton surface were measured for the beam energy smaller and larger than 50 eV, which can be found in the Supplemental Material [27]. It shows (i) for the beam energy of 38 eV, the surface is charged to a potential about −38 V to stop the beam without secondary electron emission, indicating the SEY is smaller than 1 [16,28]; and (ii) for the beam energy of 128 eV, the surface potential is only slightly negative (−6 V), and a nonmonotonic sheath is formed above the surface, which agrees with the modeling results as described in the later sections. This indicates that the surface is actually charged positively with respect to the surrounding to return some of the emitted

secondary electrons to balance the incoming electron beam current at equilibrium, indicating the SEY is larger than 1 [16,28]. The surface potential of the substrate was monitored throughout the beam energy variations, showing agreement with the SEY curve from [26].

As shown in Fig. 4, the dust mobility starts with slightly more than 50 eV where the SEY is larger than 1 and follows the SEY curve till the beam energy of 500 eV. Note that the dust mobility dies faster than the SEY curve declining for the beam energy larger than 125 eV. This is because the SEY larger than 1 is required but not sufficient for dust mobility as predicted by the modeling results of the Coulomb repulsive forces, which show good agreement with the mobility results. These results verify the role of secondary electrons in the charge enhancement and subsequent mobilization of single dust particles on a surface, as described by the PCM-SP.

In addition to the dust mobilization analysis, particle-in-cell (PIC) modeling [29] was exploited to simulate the Coulomb repulsive force (F_c). The modeling was performed in two stages. In the first stage, the experimental setup (Fig. 2) was simulated to obtain the electron flux and energy distribution function (EDF). The main features of the setup were taken into account: the sizes of elements and their disposition, the filament current, the voltages on the filament and the grounded mesh, the secondary electron yield of the kapton substrate [26]. The electron beam energy was varied in the range from 30 to 500 eV. The simulated EDF comprised the main peak of high-energy electrons from the source and the low-energy peak of secondary electrons returned to the substrate by a charge in the space. In the second stage, a SiO_2 particle resting on a kapton substrate was exposed to the bombardment of electron flux from the first stage. This simulation mainly followed the previously described one [1].

Figure 4 presents the modeled Coulomb repulsive force as a function of the electron beam energy. This plot predicts the Coulomb force to be repulsive in the entire range of energies from 50 to 300 eV with the most possible dust mobilization around 130 eV. The energy of the force peak corresponds with the maximum of secondary emission yield from kapton because it provides the biggest charge accumulation in the cavity between the substrate and the particle lying on it. The modeling results show good agreement with the experimental results, confirming that the reabsorption of emitted electrons is responsible for enhanced dust charge and subsequent mobilization, as described by the PCM-SP.

A modeled charge distribution for a 2 μm diameter particle (Fig. 5) shows negative charges on both the surfaces of the particle and the substrate within the microcavity and positive charges on the top surface of the particle with a net negative charge 1.6×10^{-15} C. These results are in agreement with the PCM-SP shown in Fig. 1. The average charge of dust particles 20 μm in diameter is

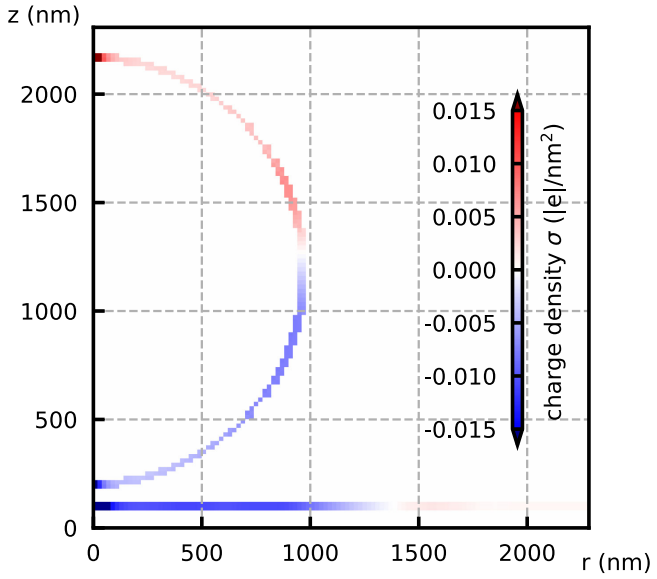

FIG. 5. 2D PIC model of a 2 μm dust particle with its charge distribution across the substrate and dust particle. A color map is shown that blue represents a negatively charged surface and red represents a positively charged surface.

estimated to be 1.6×10^{-14} C. Given an average particle separation of ~0.1 mm, the Coulomb repulsive force between the dust particles is estimated to be 0.2 nN, over 100 times less than the modeled Coulomb repulsive force of ~100 nN between the particles and the substrate surface as shown in Fig. 4. Particle-particle interactions are thus negligible in our experiments.

Furthermore, small movements of a handful of dust particles were recorded under the UV exposure (Fig. 6). As shown in previous work [16], this result cannot be explained by previous charging theories based on the sheath electric field [14,15], which is as small as 0.5 V/cm under this UV source. The maximum energy of emitted photoelectrons is ~1.7 eV, which is the difference between the photon energy (7.2 eV) and the general

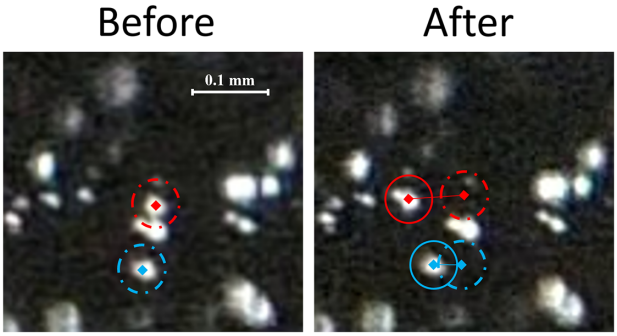

FIG. 6. Images showing dust movements (circles) under UV exposure. The dashed circles show the original positions of the dust particles and the solid circles show the positions after the movements.

work function of insulators (∼5.5 eV). The photoelectron temperature is ∼0.3 eV [30]. This is much smaller than the secondary electron temperature of ∼3 eV [28]. Therefore, the dust movement under the UV exposure is much less active than exposure to the electron beams, as shown in the experiments. The UV result of dust movements further supports the PCM-SP.

In summary, we presented the first experimental results showing that single dust particles roll or slide on a dielectric surface and are lofted from the surface due to exposure to an electron beam or UV light. A complete charging theory for single particles (PCM-SP) on a surface is developed. The PCM-SP shows that secondary electrons and/or photoelectrons emitted due to the impact of incident electrons and/or photons on a substrate surface can be recollected within microcavities formed between a dust particle and the substrate surface, resulting in the buildup of large negative charges of the dust particle and its subsequent mobilization due to Coulomb repulsion. The PCM-SP was verified with both the experiment and the modeling, in which dust mobility was tested against the electron beam energy varying from 50 to 500 eV. It was shown that the dust mobility follows the secondary electron yield curve of the substrate surface, verifying the role of secondary electrons in enhancing the charge of single dust particles on the surface as described by the PCM-SP. Small movements of dust particles under UV exposure provide further support of this charging model.

Our results made an important step into solving dust issues in semiconductor manufacturing, fusion reactors, particle accelerators, as well as lunar and asteroid exploration. Energetic electrons and/or high-energy photons exist in these scenarios, including both energetic electrons (∼70 eV) and high-energy photons (91.8 eV) in extreme ultraviolet (EUV) lithography machines [1,31], synchrotron radiation and its generated electron clouds in circular particle accelerators [4], hot electrons (100–1k eV) in fusion reactors, and solar UV radiation on airless planetary bodies [16], for example. In these scenarios, it is expected to generate sufficient secondary electrons with SEY > 1 and/or photoelectrons to charge and mobilize dust particles, as demonstrated in this work. In the future work, dust mobility for different dust, substrate surface properties, and different plasma environments will be examined to ultimately understand dust issues in these scenarios and develop mitigation solutions.

Acknowledgments—The work is supported by a contract between the Laboratory for Atmospheric and Space Physics (LASP) at the University of Colorado Boulder and ASML Netherlands B. V., and by NASA SSERVI's Institute for Modeling Plasma, Atmospheres, and Cosmic Dust (IMPACT).

[1] P. V. Krainov, V. V. Ivanov, D. I. Astakhov, V. V. Medvedev, V. V. Kvon, A. M. Yakunin, and M. A. van de Kerkhof, Dielectric particle lofting from dielectric substrate exposed to low-energy electron beam, Plasma Sources Sci. Technol. **29**, 085013 (2020).

[2] G. S. Selwyn, J. Singh, and R. S. Bennett, In situ laser diagnostic studies of plasma-generated particulate contamination, J. Vac. Sci. Technol. A **7**, 2758 (1989).

[3] P. Tolias, S. Ratynskaia, M. D. Angeli, G. D. Temmerman, D. Ripamonti, G. Riva, I. Bykov, A. Shalpegin, L. Vignitchouk, F. Brochard, K. Bystrov, S. Bardin, and A. Litnovsky, Dust remobilization in fusion plasmas under steady state conditions, Plasma Phys. Control. Fusion **58**, 025009 (2016).

[4] P. Bélanger, R. Baartman, G. Iadarola, A. Lechner, B. Lindstrom, R. Schmidt, and D. Wollmann, Charging mechanisms and orbital dynamics of charged dust grains in the LHC, Phys. Rev. Accel. Beams **25**, 101001 (2022).

[5] A. Lechner, P. Bélanger, I. Efthymiopoulos, L. Grob, B. Lindstrom, R. Schmidt, and D. Wollmann, Dust-induced beam losses in the cryogenic arcs of the CERN Large Hadron Collider, Phys. Rev. Accel. Beams **25**, 041001 (2022).

[6] B. Lindstrom, P. Bélanger, A. Gorzawski, J. Kral, A. Lechner, B. Salvachua, R. Schmidt, A. Siemko, M. Vaananen, D. Valuch, C. Wiesner, D. Wollmann, and C. Zamantzas, Dynamics of the interaction of dust particles with the LHC beam, Phys. Rev. Accel. Beams **23**, 124501 (2020).

[7] D. R. Criswell, Horizon-glow and the motion of lunar dust, in *Photon and Particle Interactions with Surfaces in Space*, edited by R. J. L. Grard, Astrophysics and Space Science Library Vol. 37 (Springer, Dordrecht, 1973), pp. 545–556, 10.1007/978-94-010-2647-5_36.

[8] J. Rennilson and D. R. Criswell, Surveyor observations of lunar horizon-glow, The Moon **10**, 121 (1974).

[9] M. S. Robinson, P. C. Thomas, J. Veverka, S. Murchie, and B. Carcich, The nature of ponded deposits on eros, Nature (London) **413**, 396 (2001).

[10] J. E. Colwell, A. A. S. Gulbis, M. Horányi, and S. Robertson, Dust transport in photoelectron layers and the formation of dust ponds on Eros, Icarus **175**, 159 (2005).

[11] B. A. Smith *et al.*, Encounter with Saturn: Voyager 1 imaging science results, Science **212**, 163 (1981).

[12] G. Morfill, E. Grün, C. Goertz, and T. Johnson, On the evolution of Saturn's "spokes": Theory, Icarus **53**, 230 (1983).

[13] B. Farr, X. Wang, J. Goree, I. Hahn, U. Israelsson, and M. Horányi, Dust mitigation technology for lunar exploration utilizing an electron beam, Acta Astro. **177**, 405 (2020).

[14] T. M. Flanagan and J. Goree, Dust release from surfaces exposed to plasma, Phys. Plasmas **13**, 123504 (2006).

[15] T. E. Sheridan and A. Hayes, Charge fluctuations for particles on a surface exposed to plasma, Appl. Phys. Lett. **98**, 091501 (2011).

[16] X. Wang, J. Schwan, H.-W. Hsu, E. Grün, and M. Horányi, Dust charging and transport on airless planetary bodies, Geophys. Res. Lett. **43**, 6103 (2016).

[17] C. Cui and J. Goree, Fluctuations of the charge on a dust grain in a plasma, IEEE Trans. Plasma Sci. **22**, 151 (1994).

[18] X. Wang, M. Horányi, and S. Robertson, Investigation of dust transport on the lunar surface in a laboratory plasma

with an electron beam, J. Geophys. Res. **115**, A11102 (2010).
[19] X. Wang, M. Horányi, and S. Robertson, Experiments on dust transport in plasma to investigate the origin of the lunar horizon glow, J. Geophys. Res. **114**, A05103 (2009).
[20] J. Schwan, X. Wang, H. W. Hsu, E. Grün, and M. Horányi, The charge state of electrostatically transported dust on regolith surfaces, Geophys. Res. Lett. **44**, 3059 (2017).
[21] A. Carroll, N. Hood, R. Mike, X. Wang, H. W. Hsu, and M. Horányi, Laboratory measurements of initial launch velocities of electrostatically lofted dust on airless planetary bodies, Icarus **352**, 113972 (2020).
[22] N. Hood, A. Carroll, R. Mike, X. Wang, J. Schwan, H. W. Hsu, and M. Horányi, Laboratory investigation of rate of electrostatic dust lofting over time on airless planetary bodies, Geophys. Res. Lett. **45**, 13,206 (2018).
[23] N. Hood, A. Carroll, X. Wang, and M. Horányi, Laboratory measurements of size distribution of electrostatically lofted dust, Icarus **371**, 114684 (2022).
[24] L. C. J. Heijmans and S. Nijdam, Dust on a surface in a plasma: A charge simulation, Phys. Plasmas **23**, 043703 (2016).
[25] C. Inguimbert, J. Pierron, M. Belhaj, and J. Puech, Extrapolated range expression for electrons down to 10 eV, in *NSREC 2016* (PORTLAND, United States, 2016), https://hal.science/hal-01372004.
[26] N. Balcon, D. Payan, M. Belhaj, T. Tondu, and V. Inguimbert, Secondary electron emission on space materials: Evaluation of the total secondary electron yield from surface potential measurements, IEEE Trans. Plasma Sci. **40**, 282 (2012).
[27] See Supplemental Material at http://link.aps.org/supplemental/10.1103/PhysRevLett.133.115301 for the vertical potential profile.
[28] X. Wang, J. Pilewskie, H. Hsu, and M. Horányi, Plasma potential in the sheaths of electron-emitting surfaces in space, Geophys. Res. Lett. **43**, 525 (2016).
[29] D. Astakhov, Numerical study of extreme-ultra-violet generated plasmas in hydrogen, Ph.D. thesis, University of Twente, Enschede, 2016.
[30] X. Wang, M. Horányi, and S. Robertson, Plasma probes for the lunar surface, J. Geophys. Res. **113**, A08108 (2008).
[31] J. Beckers, T. van de Ven, R. van der Horst, D. Astakhov, and V. Banine, Euv-induced plasma: A peculiar phenomenon of a modern lithographic technology, Appl. Sci. **9**, 2827 (2019).